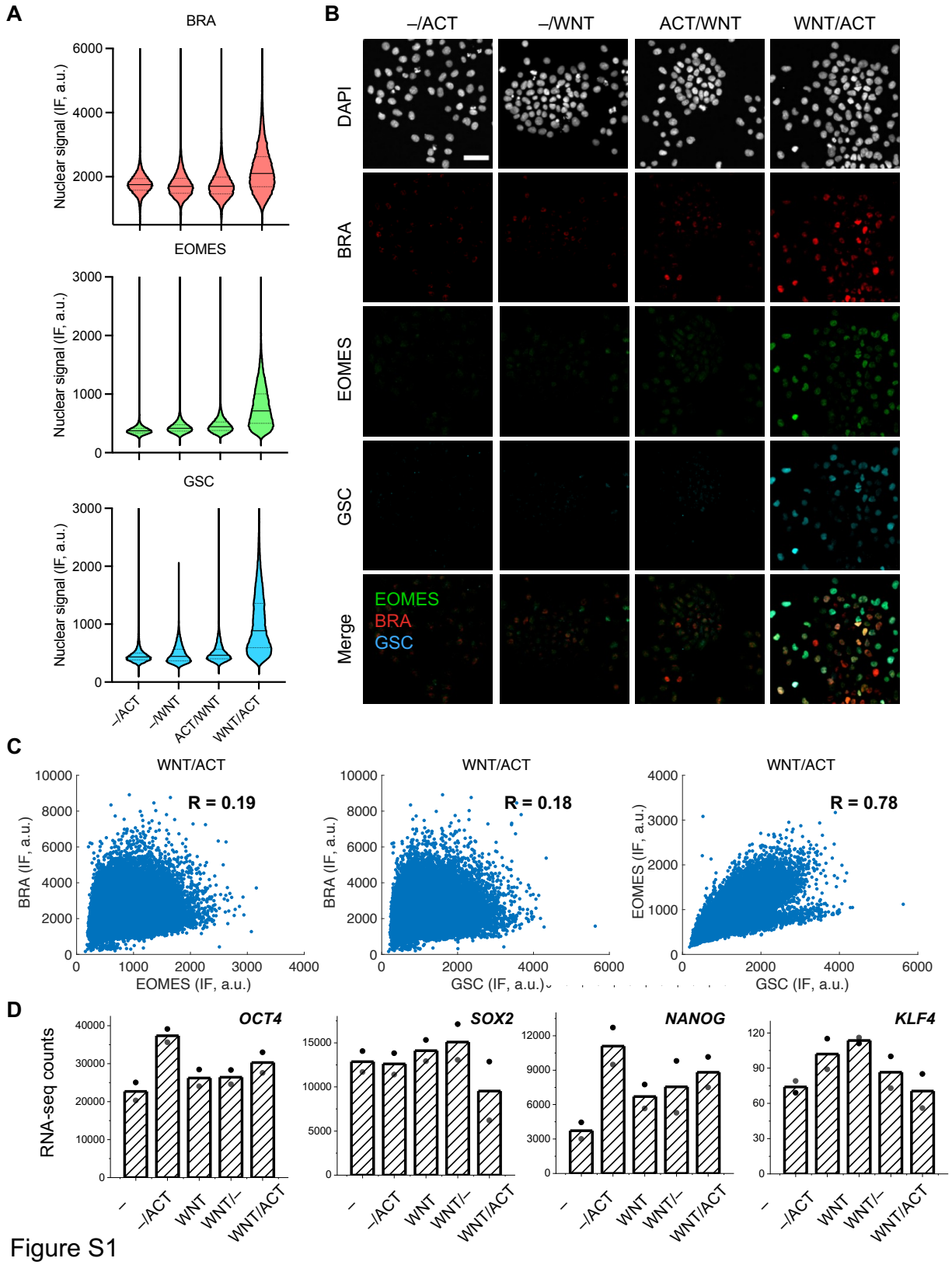

Figure S1

Fig. S1. Reverse priming does not lead to ME differentiation. A) ME differentiation requires Wnt (100 ng/mL, 24 h) priming prior to 10 ng/mL Activin treatment. The expression of the three ME genes was measured after WNT/ACT or ACT/WNT protocols and with WNT alone on the second day (–/WNT). Only the WNT/ACT protocol shows expression above background signals quantified in pluripotency conditions (–/ACT). Violin plots of the median nuclear immunofluorescence (IF) signals of three ME markers (EOMES, BRA, and GSC) quantified in single cells (n > 20,000 cells per condition). Solid line, median; Dashed lines, upper and lower quartiles. **B)** Example images corresponding to the analysis shown in (A). Scale bar, 50 μm. **C)** Scatter plots of the data shown in B from the WNT/ACT condition. EOMES and GSC are more highly correlated with each other than with BRA. R, Pearson correlation coefficient. **D)** mRNA expression levels of the pluripotency markers: *OCT4*, *SOX2*, *NANOG*, and *KLF4*. RNA counts were extracted from RNA-seq measurements (two biological replicates for each condition).

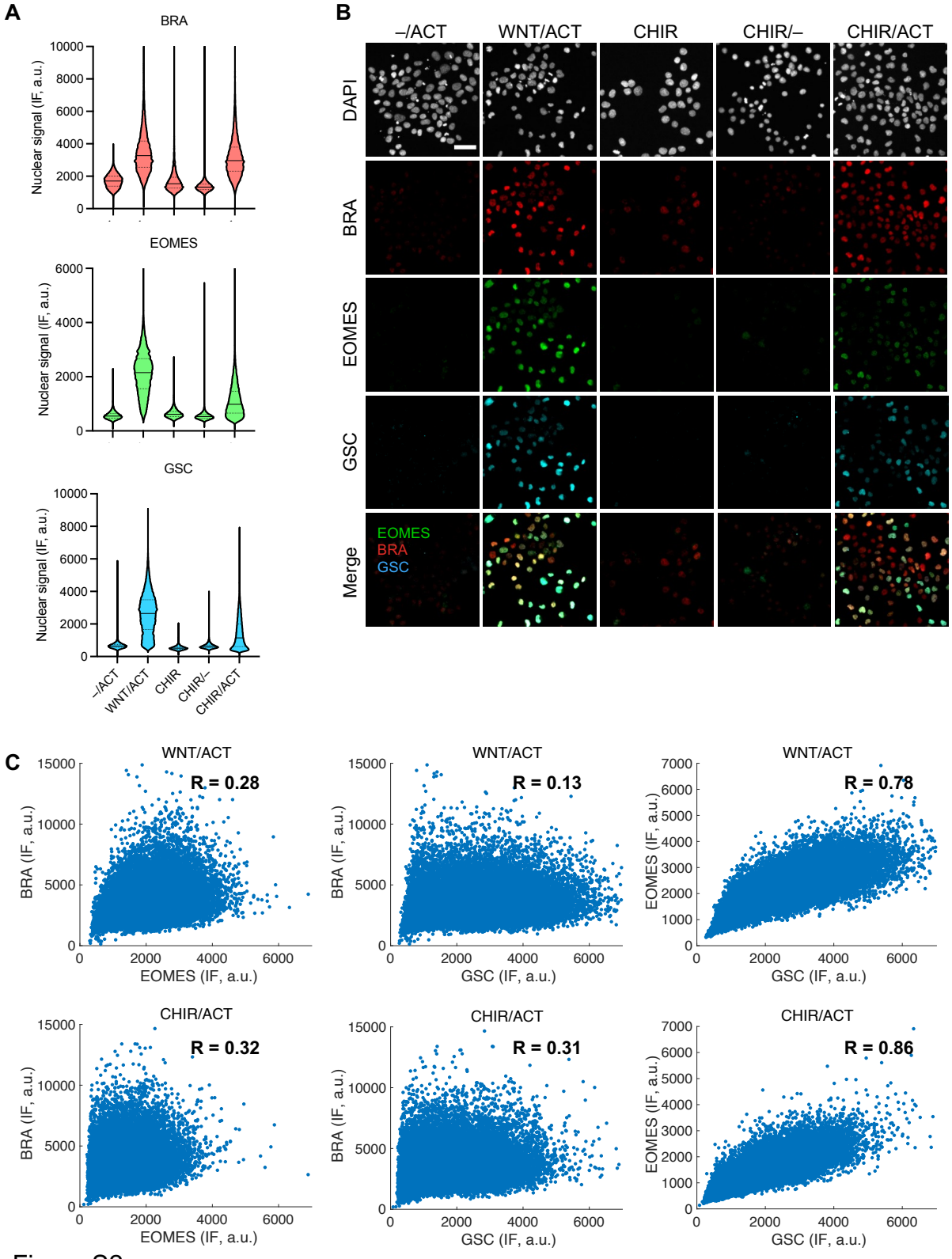

Figure S2

Fig. S2. Wnt priming is achieved with CHIR. A) WNT signaling was activated by 24h CHIR99021 (CHIR, 2.5 μM) treatment, and its effect on ME differentiation ± 10 ng/mL Activin was analyzed by immunofluorescence. Violin plots of the median nuclear immunofluorescence (IF) signals of three ME markers (EOMES, BRA, and GSC) quantified in single cells (n > 10,000 cells per condition). Solid line, median; Dashed lines, upper and lower quartiles. **B)** Example images corresponding to the analysis shown in (A). Scale bar, 50 μm. **C)** Scatter plots of the data shown in B from the ME conditions (WNT/ACT and CHIR/ACT). Similar to the data shown in Figure S1, EOMES and GSC are more highly correlated with each other than with BRA. R, Pearson correlation coefficient.

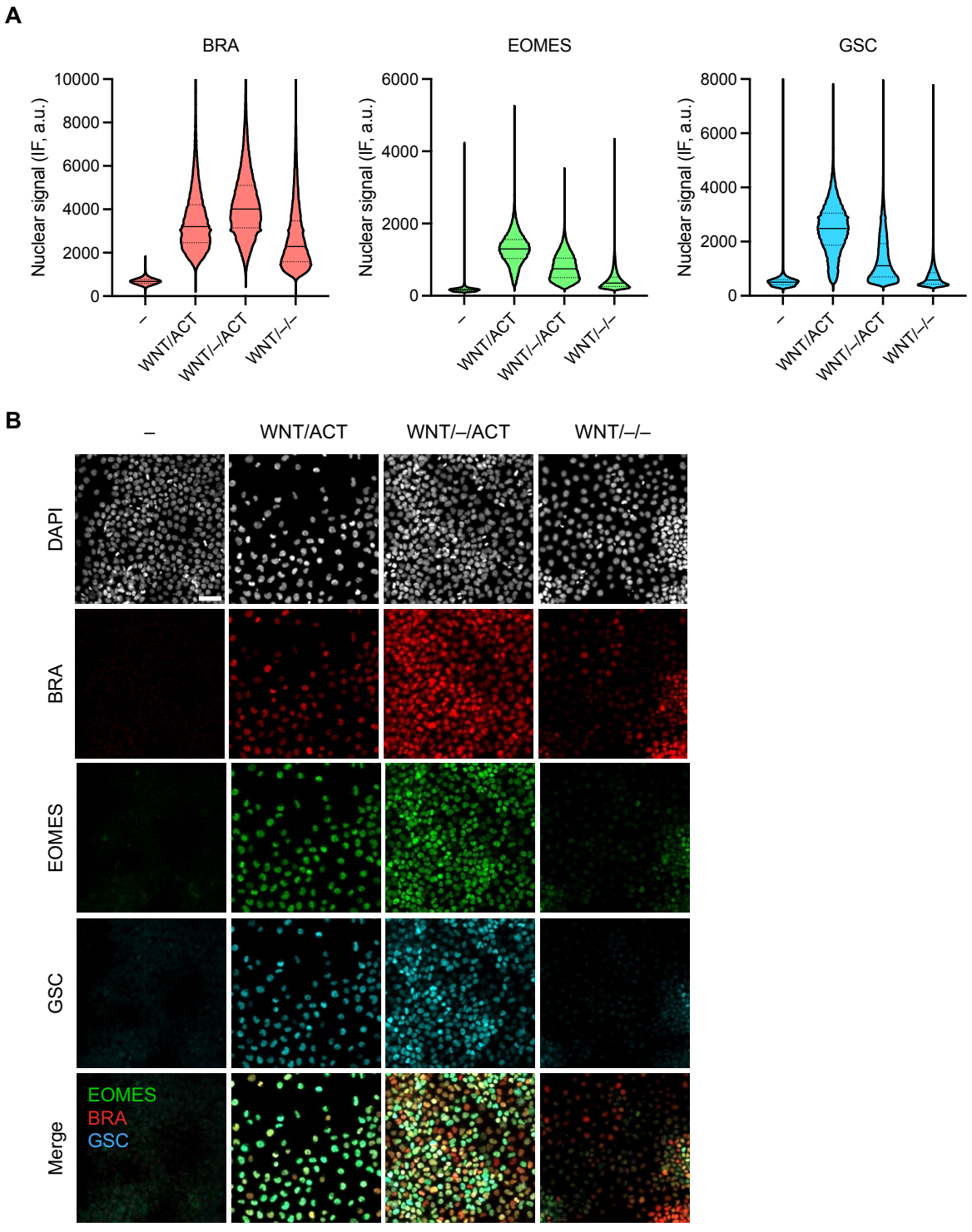

Figure S3

Fig. S3. Additional data supporting the Wnt memory phenomenon. Independent repeat of the conditions shown in Figure 1D, E in which SB was not included. **A)** Violin plots of the median nuclear immunofluorescence (IF) signal for three ME markers (BRA, EOMES, and GSC) quantified in single cells (n > 40,000 cells per condition). Solid line, median; Dashed lines, upper and lower quartiles. **B)** Example images corresponding to the analysis shown in (A). Scale bar, 50 μm.

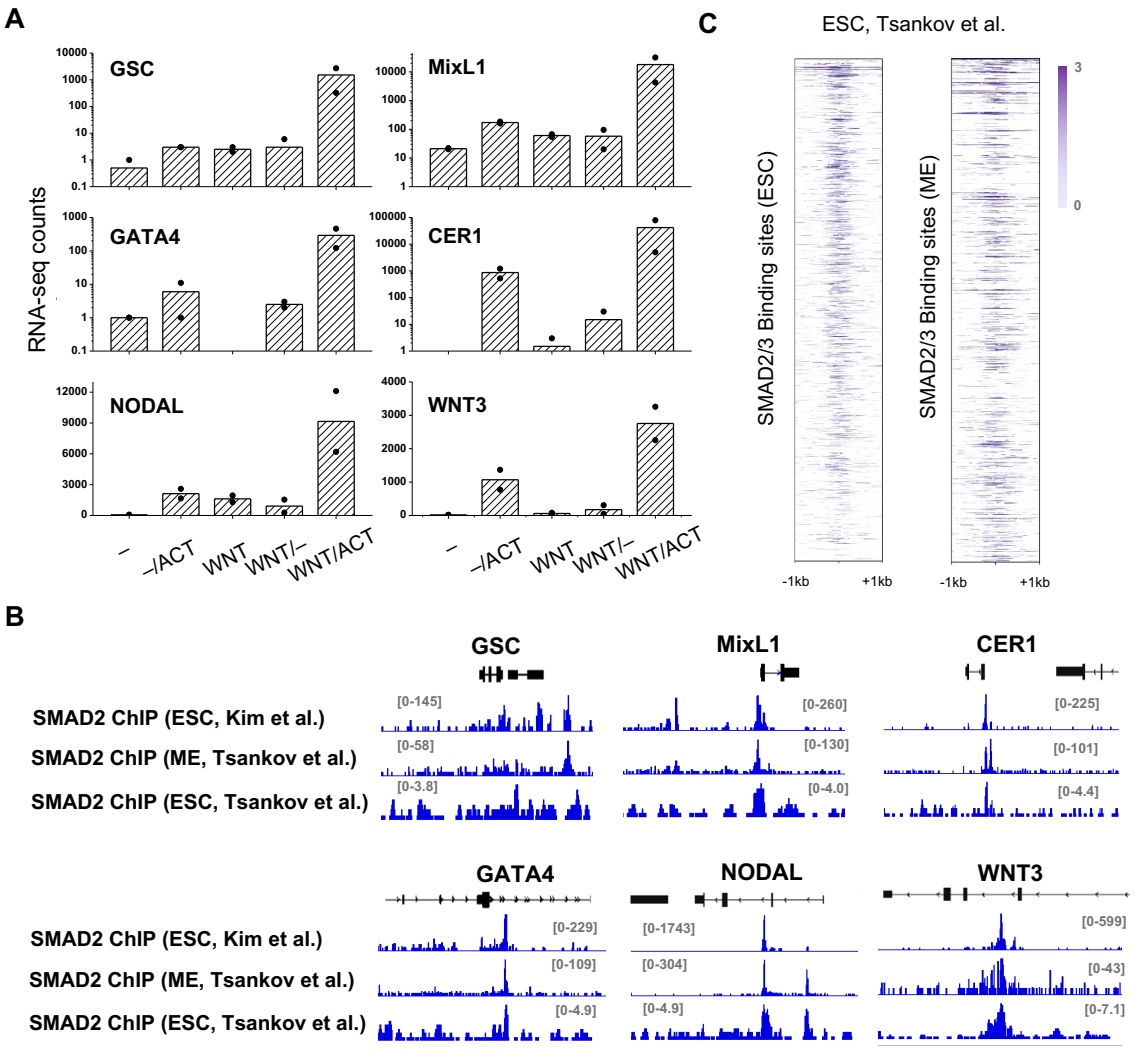

Fig. S4. Additional data supporting Figure 2A. A) mRNA expression levels of the genes shown in Figure 2A. RNA counts were extracted from RNA-seq measurements (two biological replicates for each condition). All genes show significantly higher expression in the WNT/ACT condition relative to all other conditions. **B)** Example tracks of SMAD2 ChIP-seq datasets, including the Tsankov et al. ESC dataset. **C)** Heatmap of the Tsankov et al. ESC ChIP-seq data at SMAD2/3 binding sites detected from Kim et al. ESC data (left) or from Tsankov et al. ME data (right).

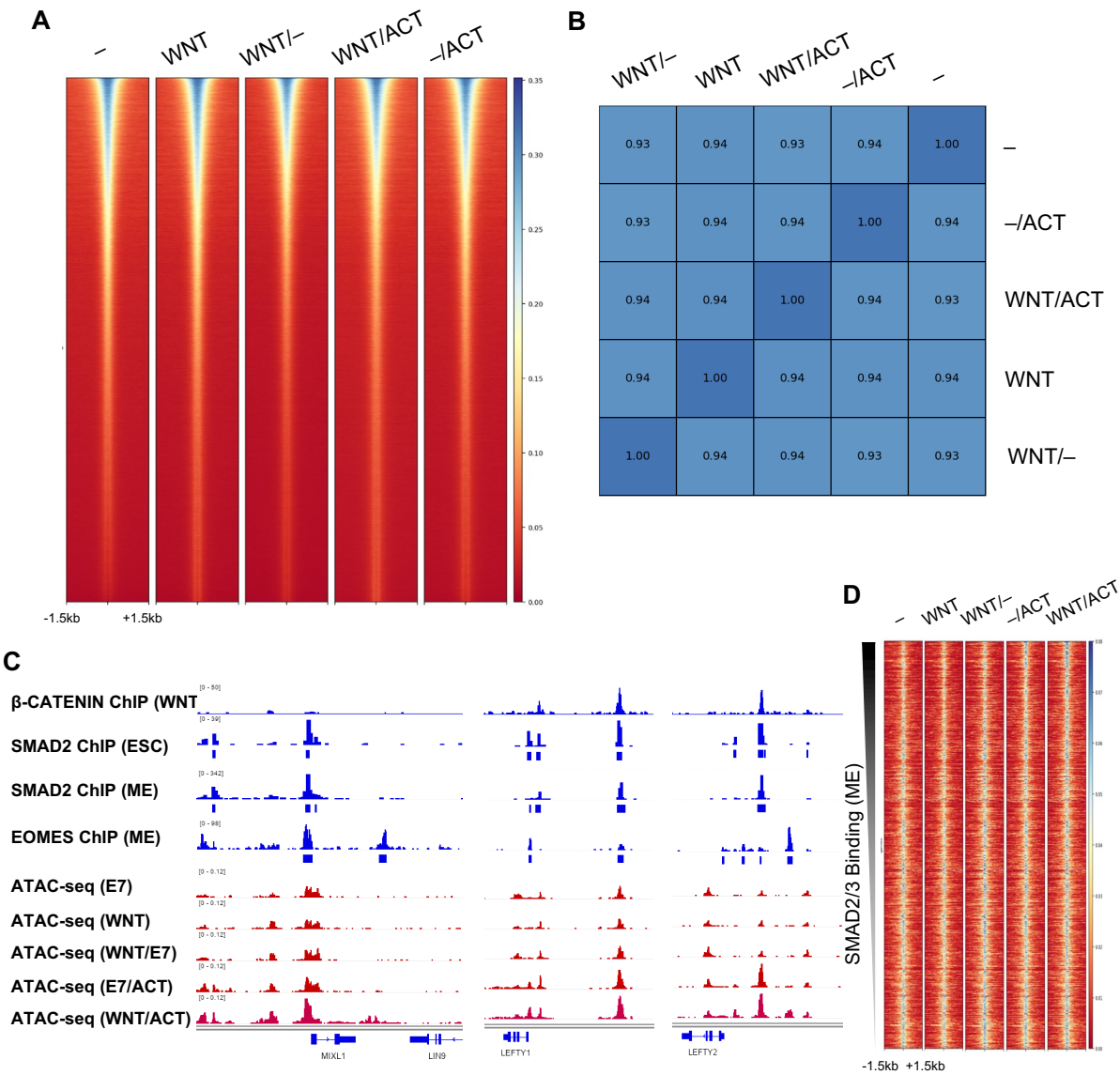

Figure S5

Fig. S5. ATAC-seq signals remain largely unchanged after WNT and/or Activin treatment. A) Heatmap of ATAC-seq peaks measured in five conditions as indicated at the top. The peak regions called in both replicates from each condition were combined and sorted in descending order based on their intensities in the E7 condition (–). All five heatmaps were plotted using the same sorted regions. The similarity of these plots indicates that there is no global rearrangement of open chromatin regions. **B)** Spearman rank-order correlations among the five ATAC-seq datasets are all > 0.93. **C)** β-CATENIN, SMAD2, and EOMES ChIP-seq, as well as ATAC-seq data near *MIXL1* and *GATA4* genes. The enhanced ATAC-seq peaks in WNT/ACT overlap with the ChIP-seq peaks of some of these factors. **D)** Same as in Figure 3D except that that SMAD2/3 binding peaks were extracted from the ChIP-seq data in ME cells.

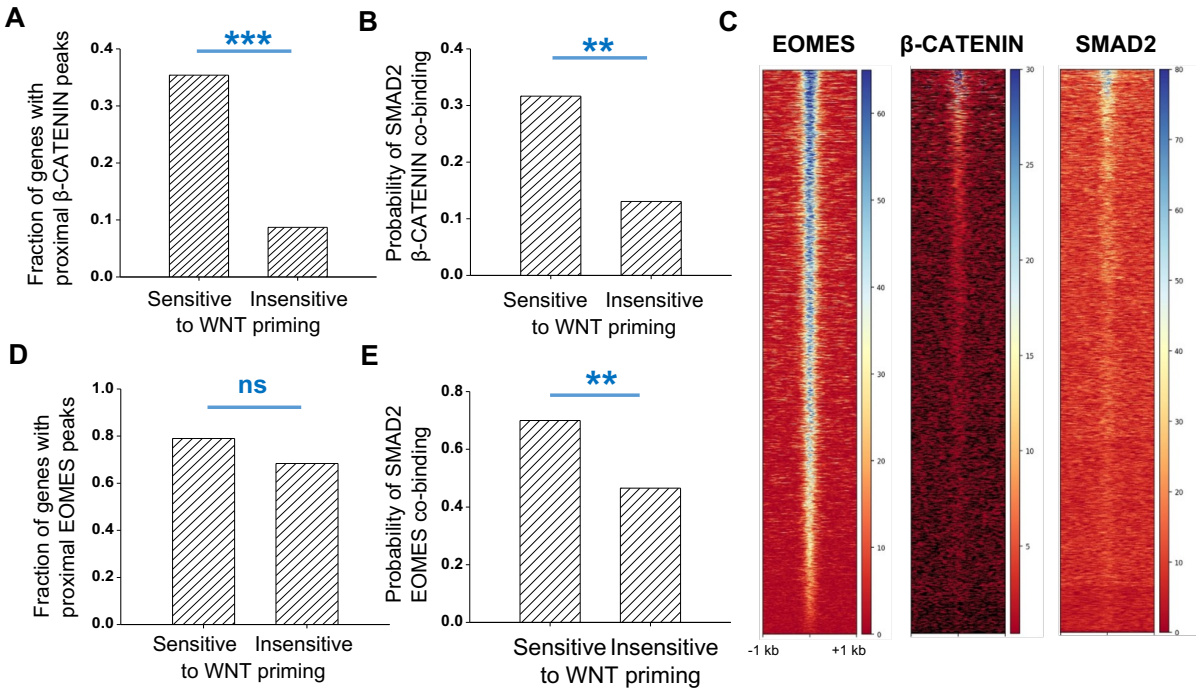

Fig. S6. Binding of β-CATENIN and EOMES to WNT-primed genes. A) Fraction of genes that are proximal to β-CATENIN ChIP-seq peaks, i.e., at least one β-CATENIN ChIP-seq peak can be found over within TSS ± 5kb. This fraction is compared among genes that are WNT-primed, and those that are not WNT-primed (*P<0.05, **P< 0.01, ***P<0.001, ns: not significant). **B)** Fraction of SMAD2/3 sites that co-localize with β-CATENIN sites. For each gene, within the range of TSS ± 5kb, we looked for SMAD2/3 and β-CATENIN ChIP peaks that are within 500 bp (co-localized peaks). The probability is calculated as the number of genes that contain co-localized peaks divided by the number of genes that contain SMAD2/3 peaks. **C)** Sorted ChIP-seq signals of β-CATENIN, SMAD2, and EOMES at the WNT/ACT enhanced ATAC-seq peaks. Most of these sites bind to EOMES, but not β-CATENIN or SMAD2. **D–E)** Same as in (A) and (B) except for EOMES.

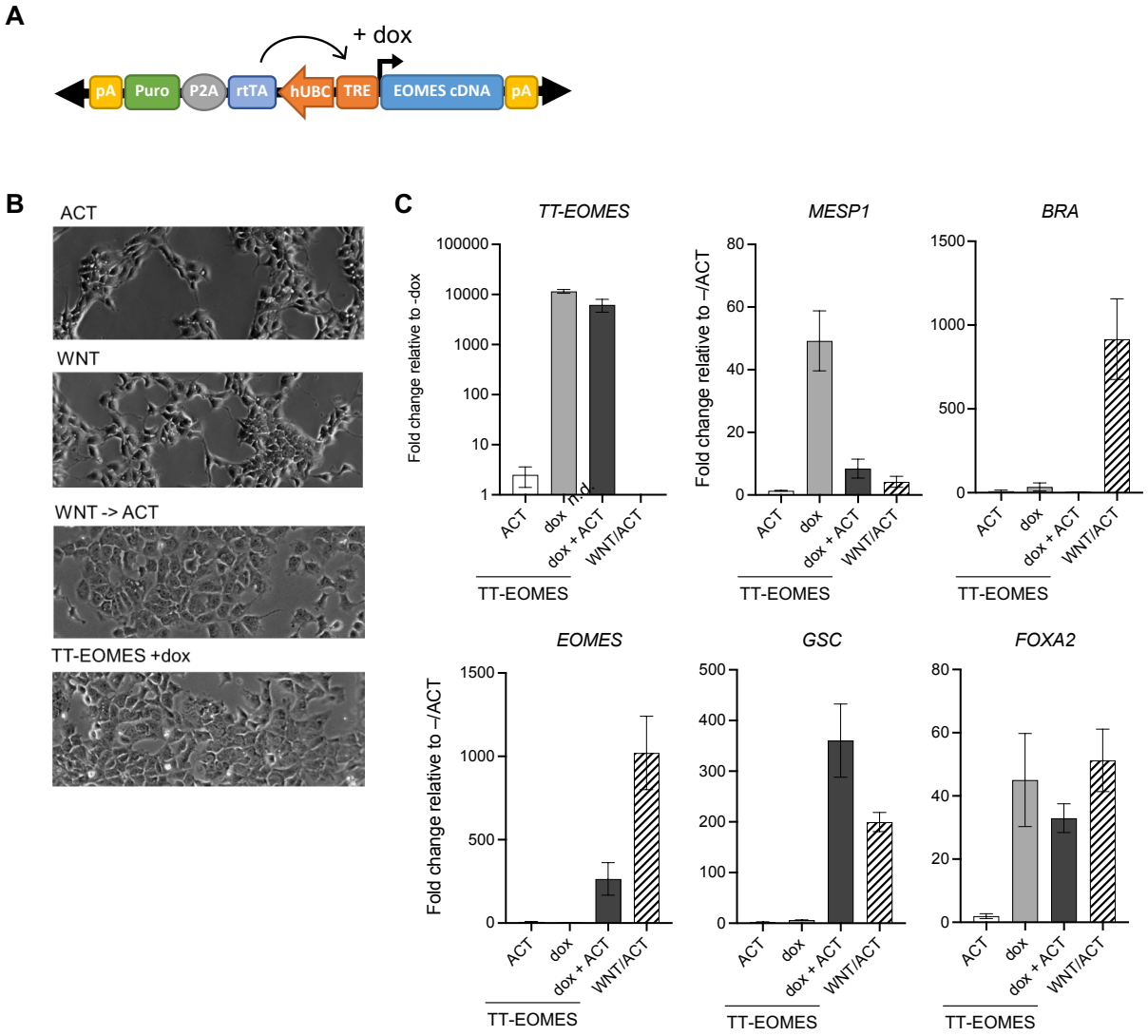

Figure S7

Fig. S7. Generation of a dox-inducible EOMES hESC line. A) Construct integrated into hESCs to induce exogenous EOMES expression with doxycycline (dox). **B)** Phase contrast images showing that dox treatment of the TT-EOMES line induces morphological changes that are similar to those observed with WNT/ACT treatment of the unmodified parental line. Cells retain a pluripotent morphology with WNT or Activin only. **C)** TT-EOMES hESCs were treated with 24 h Activin (10 ng/mL), 48 h dox (1 µg/mL), or 48 h dox (1 µg/mL) + Activin (10 ng/mL). Expression levels after standard WNT/ACT treatment of the unmodified parental line are shown for comparison. Expression in each sample was normalized to GAPDH and then to the pluripotency levels in the parental line (–/ACT) or in the case of exogenous EOMES expression (*TT-EOMES*), to the levels in the absence of dox. Similar to what was reported previously, EOMES expression induces the marker of cardiac mesoderm, *MESP1*, and Activin treatment reduces *MESP1* expression. Error bars represent the standard deviation over technical replicates. n.d., not detected.

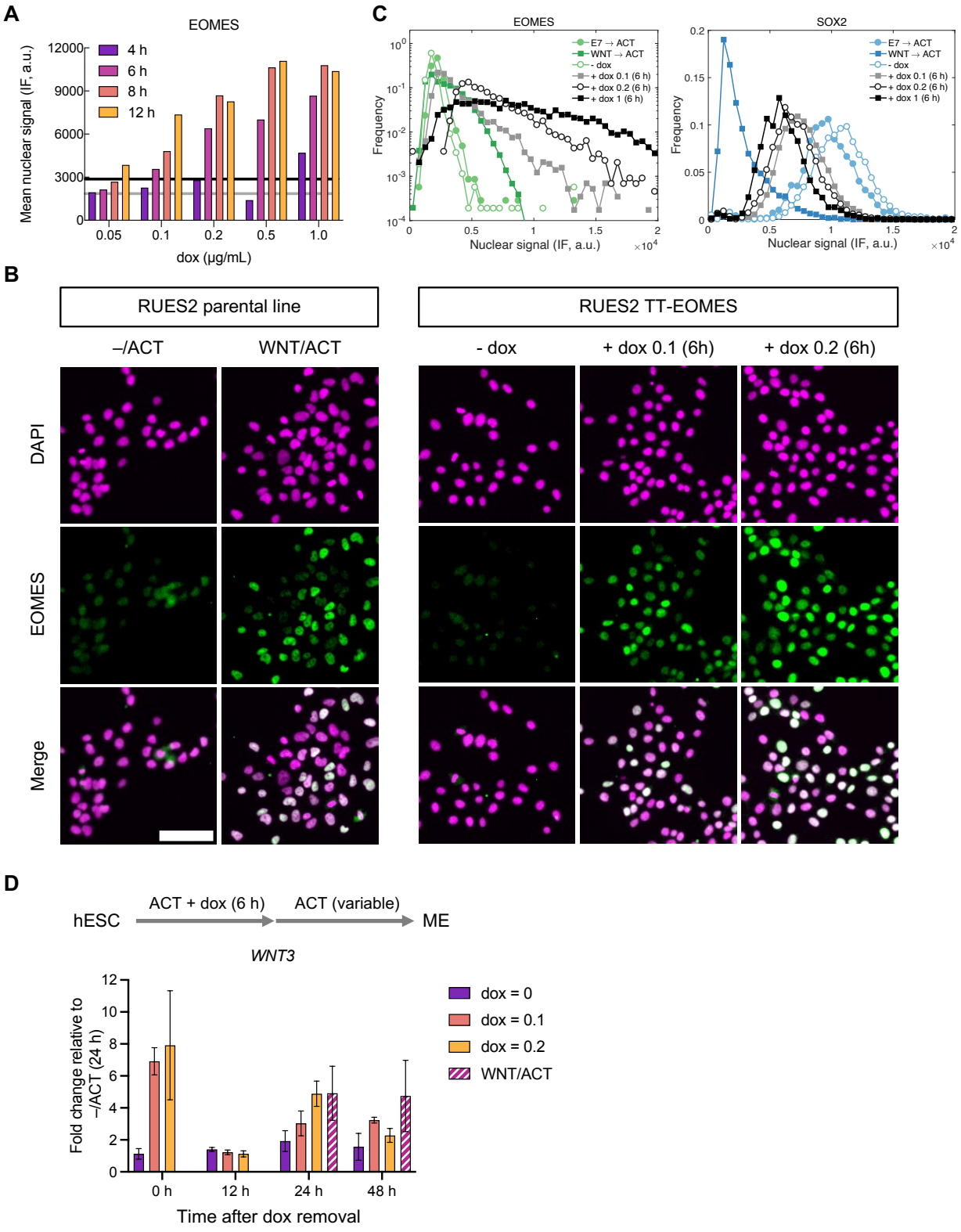

Figure S8

Fig. S8. Titration of TT-EOMES expression to achieve endogenous protein levels. **A)** EOMES expression in a clonal TT-EOMES (isoform 1) hESC line induced with different dox levels plotted along the x-axis. Expression was analyzed by immunofluorescence at different time points after dox treatment with an EOMES antibody that recognizes both the exogenous and endogenous protein. The bars show the mean expression level per cell. The mean expression in the unmodified parental line after WNT/ACT treatment (black line) and the modified line in the absence of dox (gray line) are shown for reference. The median nuclear signal was quantified in n > 2000 signal cells per condition. **B)** Example images corresponding to the analysis shown in (B) for – /ACT, WNT/ACT, and 6h dox 0.1 and 0.2 μg/mL. Scale bar, 100 μm. **C)** Histograms corresponding to the data in (A) and (B) at 6h dox treatment along with the corresponding SOX2 data. **D)** *WNT3* mRNA expression for the same experimental procedure in Figure 7A. Cells were collected at 0, 12, 24, and 48h during the Activin phase for RT-PCR measurements. Data represents the mean fold change relative to pluripotency levels in the parental line (–/ACT). Error bars represent the standard deviation over technical replicates.

Table S1. Differentially expressed genes and k-means clustering results

Click here to download Table S1

Table S2. Smad2 target genes from Yoney et al. (2018)

Click here to download Table S2

Table S3. AME results for WNT/ACT enhanced peaks

Motif	p value	adjusted p value	TP thresh	TP (%)
EOMES_HUMAN.H11MO.0.D	2.42E-20	3.15E-17	1.39	70 (81.4%)
IRF3_HUMAN.H11MO.0.B	2.30E-13	2.99E-10	1.37	66 (76.7%)
KLF1_HUMAN.H11MO.0.A	6.96E-13	9.05E-10	7.87	33 (38.4%)
BRAC_HUMAN.H11MO.1.B	1.30E-12	1.69E-09	6.51	25 (29.1%)
KLF5_HUMAN.H11MO.0.A	2.84E-12	3.70E-09	4.72	45 (52.3%)
E2F7_HUMAN.H11MO.0.B	4.07E-12	5.29E-09	4.53	37 (43.0%)
BC11A_HUMAN.H11MO.0.A	6.86E-12	8.92E-09	6.06	43 (50.0%)
SP4_HUMAN.H11MO.0.A	9.76E-12	1.27E-08	3.92	47 (54.7%)
IRF1_HUMAN.H11MO.0.A	1.22E-11	1.59E-08	1.12	44 (51.2%)
KLF3_HUMAN.H11MO.0.B	3.84E-11	5.00E-08	7.03	31 (36.0%)
TBX5_HUMAN.H11MO.0.D	6.28E-11	8.16E-08	6.71	23 (26.7%)
STAT2_HUMAN.H11MO.0.A	1.80E-10	2.33E-07	3.4	32 (37.2%)
MAZ_HUMAN.H11MO.0.A	4.66E-10	6.05E-07	12.46	44 (51.2%)
STAT1_HUMAN.H11MO.1.A	5.62E-10	7.31E-07	1.39	55 (64.0%)
IRF8_HUMAN.H11MO.0.B	9.25E-10	1.20E-06	7.9	26 (30.2%)
HTF4_HUMAN.H11MO.0.A	1.07E-09	1.39E-06	2.94	48 (55.8%)
TBR1_HUMAN.H11MO.0.D	1.75E-09	2.28E-06	8.33	19 (22.1%)
TBX1_HUMAN.H11MO.0.D	3.49E-09	4.53E-06	15.8	22 (25.6%)
WT1_HUMAN.H11MO.0.C	6.10E-09	7.93E-06	10.33	32 (37.2%)
ZBT17_HUMAN.H11MO.0.A	1.41E-08	1.83E-05	2.73	65 (75.6%)
TBX21_HUMAN.H11MO.0.A	1.62E-08	2.10E-05	5.3	22 (25.6%)
KLF15_HUMAN.H11MO.0.A	2.10E-08	2.73E-05	6.92	37 (43.0%)
SP2_HUMAN.H11MO.0.A	3.38E-08	4.40E-05	1.59	40 (46.5%)
ZN263_HUMAN.H11MO.0.A	4.05E-08	5.26E-05	2.71	50 (58.1%)
ZN770_HUMAN.H11MO.0.C	4.44E-08	5.77E-05	4.27	33 (38.4%)
SP4_HUMAN.H11MO.1.A	5.08E-08	6.60E-05	4.45	38 (44.2%)
ITF2_HUMAN.H11MO.0.C	5.35E-08	6.96E-05	3.02	46 (53.5%)
ETV5_HUMAN.H11MO.0.C	6.17E-08	8.02E-05	1.86	72 (83.7%)
EGR1_HUMAN.H11MO.0.A	6.71E-08	8.72E-05	4.65	33 (38.4%)
IRF4_HUMAN.H11MO.0.A	7.06E-08	9.17E-05	9.21	23 (26.7%)
TBX3_HUMAN.H11MO.0.C	8.94E-08	1.16E-04	2.53	51 (59.3%)
KLF4_HUMAN.H11MO.0.A	1.14E-07	1.49E-04	2.23	38 (44.2%)
ETS2_HUMAN.H11MO.0.B	1.29E-07	1.67E-04	1.82	74 (86.0%)
VEZF1_HUMAN.H11MO.0.C	1.37E-07	1.79E-04	13.39	41 (47.7%)
LYL1_HUMAN.H11MO.0.A	1.68E-07	2.18E-04	1.47	74 (86.0%)
PATZ1_HUMAN.H11MO.0.C	1.77E-07	2.30E-04	1.47	62 (72.1%)
SP3_HUMAN.H11MO.0.B	1.92E-07	2.50E-04	1.26	57 (66.3%)
ZN467_HUMAN.H11MO.0.C	2.23E-07	2.90E-04	1.95	52 (60.5%)
TBX15_HUMAN.H11MO.0.D	2.89E-07	3.76E-04	11.12	28 (32.6%)

Table S4. Primer Sequences

Set	Name	Sequence
EOMES RT-PCR	EOMES_F	gtatagtaaagacacctcaaaaggc
	EOMES_3UTR_R	aagtccatctgcaaaaagttagc
	Exo_polyA_R	ACCTCTACAAATGTGGTATGGC
Smad2 ChIP peaks	GSC_ChIP_F	GGGTCACCAATGGGGATTCA
	GSC_ChIP_R	CGCAGGAAATCAACGTGTGG
	CER1_ChIP_F	GAAGGCAGGTGGTCAGTAGC
	CER1_ChIP_R	AACCAAAGTGACGGCAGGAG
	NODAL_ChIP_F	GGCGATACCCTCAGATCCCTG
	NODAL_ChIP_R	AAGTGTCTCGCTTAACCCCG
Smad2 ChIP negative controls	NC1_ChIP_F	GGTGACCATTTTCTGGGAGTCT
	NC1_ChIP_R	ACAAGTGAAACAAAAGTATGGTGGT
	NC2_ChIP_F	ATGATCAACTGAAGAAGACTCCTG
	NC2_ChIP_R	CTCATTGAGAGATCTGTTGGCATA
Other RT-PCR	GAPDH_F	AATCCCATCACCATCTTCCA
	GAPDH_R	TGGACTCCACGACGTACTCA
	NANOG_F	TCCAACATCCTGAACCTCAGC
	NANOG_R	ACCATTGCTATTCTTCGGCCA
	OCT4_F	AAACCCACACTGCAGCAGAT
	OCT4_R	TGTGCATAGTCGCTGCTTGA
	SOX2_F	TACAGCATGATGCAGGACCA
	SOX2_R	CCGTTCATGTAGGTCTGCGA
	BRA_F	CGTTGCTCACAGACCACAG
	BRA_R	ATGACAATTGGTCCAGCCTT
	GSC_F	GAGGAGAAAGTGGAGGTCTGGTT
	GSC_R	CTCTGATGAGGACCGCTTCTG
	FOXA2_F	ATTGCTGGTCGTTTGTTGTG
	FOXA2_R	CCTCGGGCTCTGCATAGTAG
	SOX17_F	AGATGCTGGGCAAGTCGT
	SOX17_R	GCTTCAGCCGCTTCACC
	GATA4_F	AAAGAGGGGATCCAAACCAG
	GATA4_R	TTGCTGGAGTTGCTGGAAG
	GATA6_F	TCCCCCACAACACAACCTAC
	GATA6_R	TGTAGAGCCCATCTTGACCC
	MESP1_F	GAAGTGGTTCCTTGGCAGAC
	MESP1_R	TCCTGCTTGCCTCAAAGTGT
	WNT3_F	CTCGCTGGCTACCCAATTT
	WNT3_R	GAGCCCAGAGATGTGTACTGC